ORIGINAL ARTICLE

Identification of a sugar gustatory receptor and its effect on fecundity of the brown planthopper *Nilaparvata lugens*

Wei-Wen Chen[*], Kui Kang[*], Pan Yang and Wen-Qing Zhang (iD)

State Key Laboratory of Biocontrol and School of Life Sciences, Sun Yat-sen University, Guangzhou, China

Abstract In insects, the gustatory system plays a crucial role in multiple physiological behaviors, including feeding, toxin avoidance, courtship, mating and oviposition. Gustatory stimuli from the environment are recognized by gustatory receptors. To date, little is known about the function of gustatory receptors in agricultural pest insects. In this study, we cloned a sugar gustatory receptor gene, *NlGr11*, from the brown planthopper (BPH), *Nilaparvata lugens* (Stål), a serious pest of rice in Asia; we then identified its ligands, namely, fructose, galactose and arabinose, by calcium imaging assay. After injection of *NlGr11* double-stranded RNA, we found that the number of eggs laid by BPH decreased. Moreover, we found that *Nl*Gr11 inhibited the phosphorylation of adenosine monophosphate-activated protein kinase (AMPK) and promoted the phosphorylation of protein kinase B (AKT). These findings demonstrated that *Nl*Gr11 could accelerate the fecundity of BPH through AMPK- and AKT-mediated signaling pathways. This is the first report to indicate that a gustatory receptor modulates the fecundity of insects and that the receptor could be a potential target for pest control.

Key words brown planthopper; fecundity; gustatory receptors; ligands; sugar

Introduction

Animals rely on their gustatory system to detect and discriminate between different taste stimuli in their environments. In insects, the gustatory system plays a crucial role in multiple physiological behaviors, including feeding, toxin avoidance, courtship, mating and oviposition (Sato *et al.*, 2011). Gustatory stimuli from the environment are recognized by gustatory receptors and gustatory receptor neurons located in sensilla distributed on several different parts throughout the body (Scott *et al.*, 2001).

Insect gustatory receptors often possess seven-transmembrane domains, but compared to classical G-protein coupled receptors (GPCRs), the topology is reverse, with an intracellular N-terminus and an extracellular C-terminus (Clyne *et al.*, 2000; Zhang *et al.*, 2011).

Correspondence: Wen-Qing Zhang, State Key Laboratory of Biocontrol and School of Life Sciences, Sun Yat-sen University, Guangzhou 510275, China. Tel: + 86 20 39332963; fax: +86 20 39943515; email: lsszwq@mail.sysu.edu.cn

[*]These authors contributed equally to this work.

Gustatory receptors are diverse, demonstrate broad ligand selectivity for several molecules and have been classified into four clades: GR43a-like, CO_2, sugar and bitter clades (Xu *et al.*, 2012). To date, most of the published studies about gustatory receptors have focused on *Drosophila melanogaster* (Lee *et al.*, 2010; Miyamoto *et al.*, 2012; Ni *et al.*, 2013; Freeman *et al.*, 2014; Shim *et al.*, 2015). However, little is known about the function of gustatory receptors in agricultural pest insects. At present, insect sugar gustatory receptors are studied mainly in two respects. First, there is the identification of sugar gustatory receptors. With the rapid progress of genome projects focused on insect species, the identification of sugar gustatory receptors is being extended to a diverse range of insect species. The gustatory receptor families have revealed two, seven, eight, seven, two, five, eight, five and five sugar receptors in *Apis mellifera* (Robertson & Wanner, 2006), *D. melanogaster* (Jiao *et al.*, 2007), *Aedes aegypti* (Kent *et al.*, 2008), *Heliconius melpomene* (Briscoe *et al.*, 2013), *Conogethes punctiferalis* (Ge *et al.*, 2016), *Athetis dissimilis* (Dong *et al.*, 2016), *Helicoverpa armigera* (Xu *et al.*, 2016), *Aphidius gifuensis* (Kang *et al.*, 2017), and *Bombyx mori* (Guo *et al.*, 2017),

441

respectively. Second, there is the identification of their ligands. At present, most of the gustatory receptors whose ligands have been identified are sugar gustatory receptors (Dahanukar *et al.*, 2001; Sato *et al.*, 2011; Xu *et al.*, 2012; Jung *et al.*, 2015). *Dm*Gr5a, a sugar gustatory receptor from *D. melanogaster*, was the first gustatory receptor to have its ligand, trehalose, identified (Dahanukar *et al.*, 2001). The ligands of *Bm*Gr9 in *B. mori* and *Gr*43a in *D. melanogaster* were later identified (Sato *et al.*, 2011; Miyamoto *et al.*, 2012). Moreover, sugar gustatory receptors could form multimeric complexes for the detection of sugars, such as *Am*Gr1 and *Am*Gr2 of *A. mellifera*. Co-expression of *Am*Gr1 and *Am*Gr2 showed higher sensitivity to glucose and lower sensitivity to sucrose, trehalose and maltose compared with *Am*Gr1 expression alone (Jung *et al.*, 2015).

The brown planthopper (BPH), *Nilaparvata lugens* (Stål), is a serious pest of rice in Asia (Jena & Kim, 2010). In recent years, BPH has caused serious damage to rice crops. Long-distance migration, high fecundity and strong pesticide resistance are the main characteristics of BPH. In this study, we tried to establish the relationship between gustatory receptors and fecundity in BPH. First, we cloned a sugar gustatory receptor gene, *NlGr11*, from BPH and identified its ligands by calcium imaging assay. Then, we found that *Nl*Gr11 accelerated the fecundity of BPH through adenosine monophosphate-activated protein kinase (AMPK)- and protein kinase B (AKT)-mediated signaling pathways.

Materials and methods

Insect and cell lines

The *N. lugens* (BPH) populations used in this work were originally collected in Guangdong Province, China, in 2012. All BPHs were mixed reared in a walk-in chamber at $26 \pm 1°C$ under a photoperiod of 16 : 8 h (light : dark) at a relative humidity level of 80% ($\pm 10\%$) on susceptible rice seedlings (rice variety Huang Huazhan).

Spodoptera frugiperda (*Sf*9) cells were cultured in Grace's Insect Medium (Gibco, Waltham, MA, USA) supplemented with 10% inactivated fetal bovine serum (Gibco) at 27°C.

Cloning of NlGr11

Total RNA was extracted from pooled samples (1st to 5th instar nymphs and adults) using Total RNA Kit II (Omega Bio-tek, Norcross, GA, USA) following the manufacturer's instructions. One microgram of RNA was used for the first-strand complementary DNA (cDNA) synthesis by PrimeScript™ RT reagent Kit with gDNA Eraser (Takara, Kyoto, Japan). First, the sequences of open reading frames (ORFs) were cloned using 2× SuperStar PCR Mix with Loading Dye (Genstar, Beijing, China) according to the manufacturer's instructions. Subsequently, the full cDNA sequences of *NlGr11* were cloned using 5′ rapid amplification of cDNA ends (RACE) and 3′ RACE core sets (Takara). One microgram of total RNA was used for 5′ RACE or 3′ RACE cDNA synthesis following the manufacturer's instructions. Finally, nested polymerase chain reaction (PCR) was performed to obtain the 5′-end/3′-end sequence with primer pairs. All primers used for PCR are listed in Table S1. The amplification conditions were as follows: 98°C for 30 s; followed by 35 cycles of 98°C for 15 s, 55°C for 30 s (30 s/1 kb), and 72°C for 15 s; and finally, 72°C for 7 min.

Calcium imaging assay for ligand of NlGr11

The ORF of *NlGr11* was cloned using gene-specific primers (Table S1). The PCR product was digested with Hind III and EcoR I, and the digested target gene was ligated into pIZ/V5-His vector (Invitrogen, Carlsbad, CA, USA), previously digested by the same enzymes. The constructed plasmids were further sequenced to confirm the orientation and sequence. Subsequently, *Sf*9 cells were plated into 12-well plates and left to settle for approximately 20 min. Finally, the cells were transfected with 200 ng of plasmid construct pIZ/*Nl*Gr11 or pIZ/V5-His vector (negative control) and 6 μL of Fugene HD transfection reagent (Promega, Madison, WI, USA) in 100 μL of medium per well. After successful transfection, the *Nl*Gr11-*Sf*9 stable cell lines were established according to the manufacturer's instructions of pIZ/V5-His vector (Invitrogen). Briefly, the medium was removed and replaced with medium containing Zeocin (5 μg/mL) and incubated cells at 27°C. Selective medium was replaced every 3 to 4 days and the resistant cells were let to gradually grow out to confluence for a stable cell line. In this process, the concentration of Zeocin was gradually increased to 50 μg/mL and used medium containing Zeocin when maintaining stable cell lines. The methods of calcium imaging in *Nl*Gr11-*Sf*9 stable cell lines and data analysis were the same as previously described (Zhang *et al.*, 2011). The only difference was that the images were recorded every 3 s for 120 s.

dsRNA preparation and injection in BPH

Double-stranded RNA (dsRNA) was prepared as follows: the DNA template for dsRNA synthesis was

amplified with primers containing the T7 promoter sequence at both ends (Table S1), and the purified DNA template was then used to synthesize dsRNA. dsRNA was synthesized using the MEGAscript T7 High Yield Transcription Kit (Promega) following the manufacturer's instructions. Subsequently, the concentrations of *NlGr11* dsRNA (380 bp), *AMPK* dsRNA (460 bp) and *AKT* dsRNA (424 bp) were quantified with a NanoDrop 2000 instrument (Thermo Fisher Scientific, Waltham, USA). Finally, the quality and size of the dsRNA were further verified via electrophoresis in a 1% agarose gel. *GFP* dsRNA was used as a control (Pang *et al.*, 2017).

From the culture chamber, 1-day-old females were collected and anesthetized with CO_2 for 20 s. The dsRNA injection experiment was conducted as previously described (Chen *et al.*, 2013). Approximately 250 ng dsRNA was injected into the individuals. After injection, the females were reared on fresh rice plants, which were maintained in transparent polycarbonate jars measuring 15 cm in diameter and 70 cm in height. At 24 h, 48 h and 72 h after injection, RNA was extracted from five individuals to examine the gene silencing efficiency by quatitative reverse transcription PCR (qRT–PCR).

qRT-PCR analysis

Total RNA isolation and cDNA synthesis were performed as previously described. qRT-PCR was performed using a Light Cycler 480 (Roche Diagnostics, Basel, Switzerland) with the SYBR® FAST Universal qPCR Kit (KAPA, Woburn, MA, USA) following the manufacturer's instructions. Each reaction mixture included 1 μL of cDNA template equivalent to 1 ng of total RNA, 0.3 μL of each primer (10 μmol/L) and 5 μL SYBR mix in a total volume of 10 μL. Reactions were performed in triplicate for each sample; three biological replicates and three reactions for each biological replicate were performed. The gene expression levels were normalized to the expression level of *N. lugens* β-actin (Chen *et al.*, 2013). The specific primers used for qRT-PCR are listed in Table S1. The amplification conditions were as follows: 95°C for 5 min, followed by 45 cycles of 95°C for 10 s, 60°C for 20 s and 72°C for 20 s.

Western blot

Protein was extracted 72 h after dsRNA injection. Total protein from whole bodies was extracted from seven females, fat bodies and ovaries were extracted from 20 females in each of three replicates performed.

Whole bodies or fat bodies or ovaries were lysed in 1× Passive Lysis Buffer. The homogenate was centrifuged at 12 000 × *g* at 4°C for 15 min, and protein contents in the supernatant were measured by the Bradford method. The Western blot technique was modified according to previously described methods (Mitsumasu *et al.*, 2008). In this study, 30 μg of total protein were separated on a 10% SDS–PAGE and transferred to poly(vinylidene difluoride) membranes (0.45 μm, Millipore, Billerica, MA, USA), and the membranes were immunoblotted with anti-*Nl*Gr11 (1 : 500, Abmart, Shanghai, China), anti-*Nl*Vg (vitellogenin, 1 : 500, Abmart), anti-*Nl*VgR (vitellogenin receptor, 1 : 500, Abmart), anti-AMPKα (1 : 1000, Abcam, Cambridge, UK), anti-phospho-AMPKα (1 : 1000, CST, Boston, MA, USA), anti-AKT (1 : 1000, CST), anti-phospho-AKT (1 : 1000, CST) and anti-β-actin (1 : 4000, Abcam). Secondary antibody was immunoglobulin G (IgG) goat anti-rabbit antibody conjugated to horseradish peroxidase (HRP) (1 : 20 000, Trans, Beijing, China) or IgG goat anti-mouse antibody conjugated to HRP (1 : 10 000, Trans). The membranes were visualized using electrochemiluminescence (Millipore) and Image Lab (Bio-Rad, Hercules, CA, USA). The protein bands were quantified by importing the images into ImageJ analysis software (Wayne Rasband, National Institutes of Health, Bethesda, MD, USA).

Measurement of fecundity

For fecundity bioassay, each 1-day-old female injected with dsRNA was paired with two untreated males and then transferred to fresh rice plants. Thirty replicates were performed for the treatment, and the control consisted of 30 pairs of adults. The number of eggs was counted under a microscope 7 days later, and these pairs of adults were then transferred to new rice plants for another 8 days of oviposition observation.

Statistical analysis

For the statistical analysis of the qRT-PCR results, the relative expression and $2^{-\Delta\Delta Ct}$ values were calculated as previously described (Chen *et al.*, 2013). All mRNA levels were normalized relative to the β-actin mRNA levels (Pang *et al.*, 2017). All results are expressed as means + SEM, and the differences between two groups were analyzed using *t*-tests. The differences between multiple groups were analyzed using one-way analysis of variance followed by Duncan's multiple range test for multiple comparisons. Statistical differences were considered significant at $P < 0.05$ (marked *) and very significant at $P < 0.01$ (marked **).
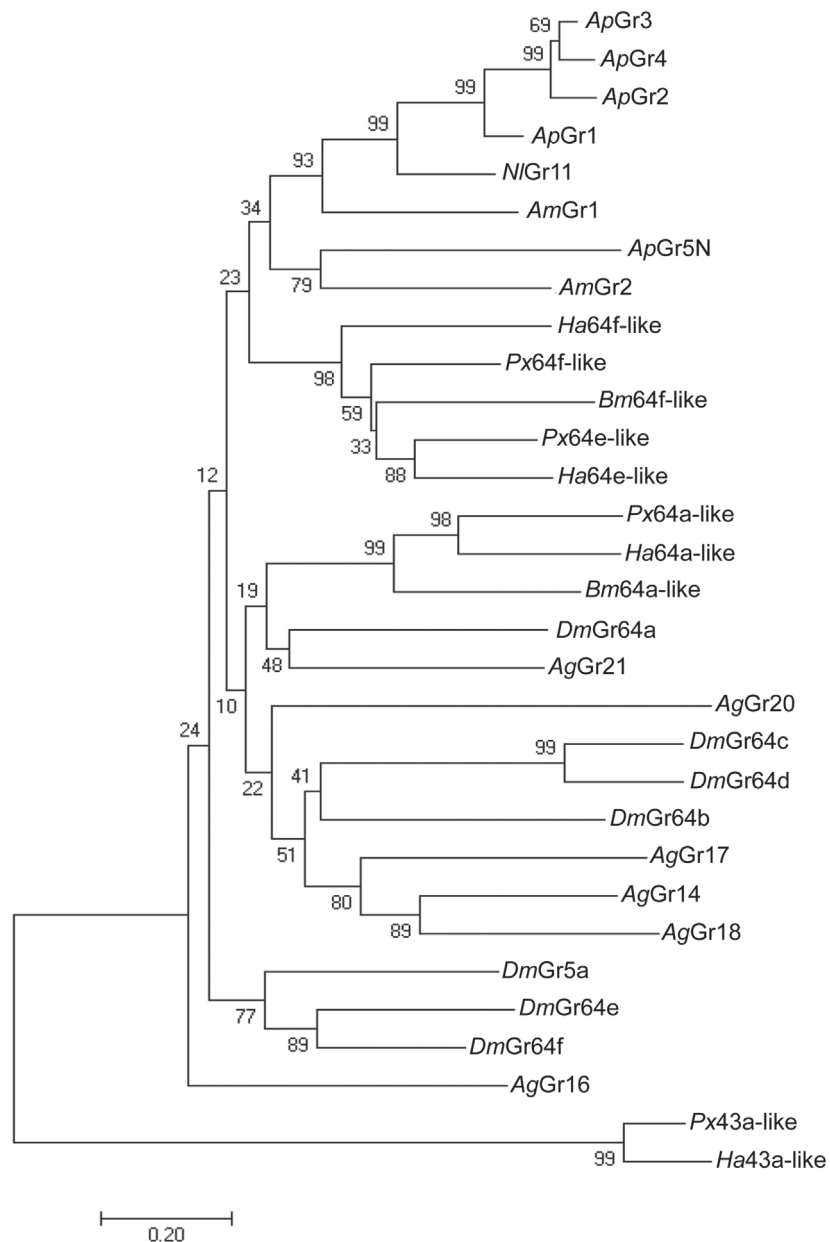
Fig. 1 Phylogenetic analysis of sugar gustatory receptor genes from insects. The analyzed genes included: *Ap*, *Acyrthosiphon pisum*, *Ap*Gr1 (XP_001942787), *Ap*Gr2 (XP_016662920), *Ap*Gr3 (XP_008186707), *Ap*Gr4 (XP_003246994), *Ap*Gr5N (XP_016660313); *Am*, *Apis mellifera*, *Am*Gr1 (XP_006567793), *Am*Gr2 (XP_397125); *Dm*, *Drosophila melanogaster*, *Dm*Gr5a (NP_511050), *Dm*Gr64a (NP_728920), *Dm*Gr64b (NP_728921), *Dm*Gr64c (NP_523913), *Dm*Gr64d (NP_001027105), *Dm*Gr64e (NP_001027106), *Dm*Gr64f (NP_728924); *Ag*, *Anopheles gambiae*, *Ag*Gr14 (XP_316432), *Ag*Gr16 (XP_316432), *Ag*Gr17 (XP_307763), *Ag*Gr18 (XP_307764), *Ag*Gr20 (XP_003436428), *Ag*Gr21 (XP_307768); *Px*, *Papilio xuthus*, *Px*43a-like (XP_013181119.1), *Px*64a-like (XP_013168118.1), *Px*64e-like (XP_013168119.1), *Px*64f-like (XP_013163369.1); *Bm*, *Bombyx mori*, *Bm*64a-like (XP_021208998.1), *Bm*64f-like (XP_021180835.1); *Ha*, *Helicoverpa armigera*, *Ha*43a-like (XP_021196329.1), *Ha*64a-like (XP_021182097.1), *Ha*64e-like (XP_021201486.1), *Ha*64f-like (XP_013163369.1).

Results

Molecular cloning and expression patterns of NlGr11

Using the transcriptome database of BPH established by our laboratory (unpublished), we gained several homology fragments through alignment with known insect sugar gustatory receptor sequences. One of the fragments, named *Nl*Gr11, was chosen for further study. Thus, the sequence of its ORF was amplified by PCR with gene-specific primers. After RACE experiments were conducted, the complete sequence of *NlGr11* (GenBank accession no. MG211370) was obtained (1584 bp), consisting of a 105 bp 5-untranslated region (UTR), a 465 aa ORF with seven predicted transmembrane domains and an 80 bp 3′ UTR (Fig. S1). The predicted molecular weight of the mature protein was 52.8 kDa, with an isoelectric point (pI) of 8.44. In addition, using MEGA software and test-neighbor-joining method, we performed a phylogenetic analysis of *Nl*Gr11 with 30 other insect sugar gustatory receptors (Fig. 1). The results showed that *Nl*Gr11 has higher homology with *Ap*Gr1, *Ap*Gr2, *Ap*Gr3 and *Ap*Gr4.

Using gene-specific primers, we performed a qRT-PCR analysis on RNA isolated from different stages of BPH and various tissues of 1-day-old females. We found that *NlGr11* was widely expressed in different stages and tissues, but it was mainly expressed in the midgut (Fig. 2B). Moreover, the mRNA levels of *NlGr11* were higher in female adults than in male adults (Fig. 2A), suggesting that *NlGr11* may be related to the fecundity of BPH.

Ligand determination for NlGr11 by calcium imaging assay

Because *Nl*Gr11 was predicted to be a sugar gustatory receptor, we selected 12 types of sugar for the calcium imaging assay: fructose, glucose, maltose, sucrose, galactose, arabinose, xylose, trehalose, ribose, sorbose, maltotriose and melezitose (purchased from Beijing Dingguo Changsheng Biotech. Co. Ltd, purity ≥ 98.5%). After successfully establishing the *Nl*Gr11-*Sf*9 stable cell lines (Fig. S2), we examined the effects of candidate sugars on the *Nl*Gr11 expressed in *Sf*9 cells by calcium imaging assay.

The results showed that only fructose, glucose, galactose, arabinose and xylose caused an increase in ΔF (Fig. 3A; Fig. S3). In addition, we added different concentrations of those five sugars into the same dish of *Nl*Gr11-*Sf*9 cells every 30 s and into different dishes of *Nl*Gr11-*Sf*9 cells to further determine the ligands. We observed that only fructose, galactose and arabinose resulted in dose-dependent responses at concentrations ranging from 5 mmol/L to 100 mmol/L and showed a saturatable response at 50 mmol/L (Fig. 3B, C). These results showed that fructose, galactose and arabinose are ligands of *Nl*Gr11.

Effect of NlGr11 on fecundity of BPH

By injecting *NlGr11*dsRNA into 1-day-old females, using gene-specific primers, we performed a qRT-PCR
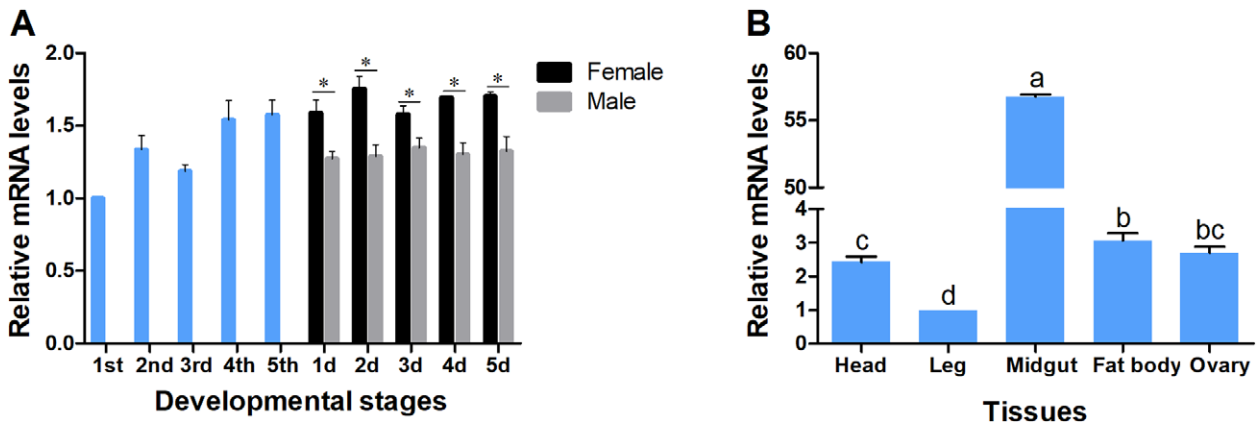

Fig. 2 Spatio-temporal expression pattern of *NlGr11* gene. (A) The messenger RNA (mRNA) levels of *NlGr11* in different developmental stages. 1st–5th, first to fifth instar nymph. 1d–5d, first to fifth day female or male adults. All mRNA levels were normalized relative to the *β*-actin mRNA levels. The mRNA level of 1st-instar nymphs was set to 1. The data represent means + SEM ($n = 3$), *$P < 0.05$, *t*-test. (B) The mRNA levels of *NlGr11* in the different tissues of 1-day-old females. All mRNA levels were normalized relative to the *β*-actin mRNA levels. The mRNA level of legs was set to 1. The data represent means + SEM ($n = 3$), different lower-case letters above columns represent significant differences ($P < 0.05$, Duncan's multiple range test).
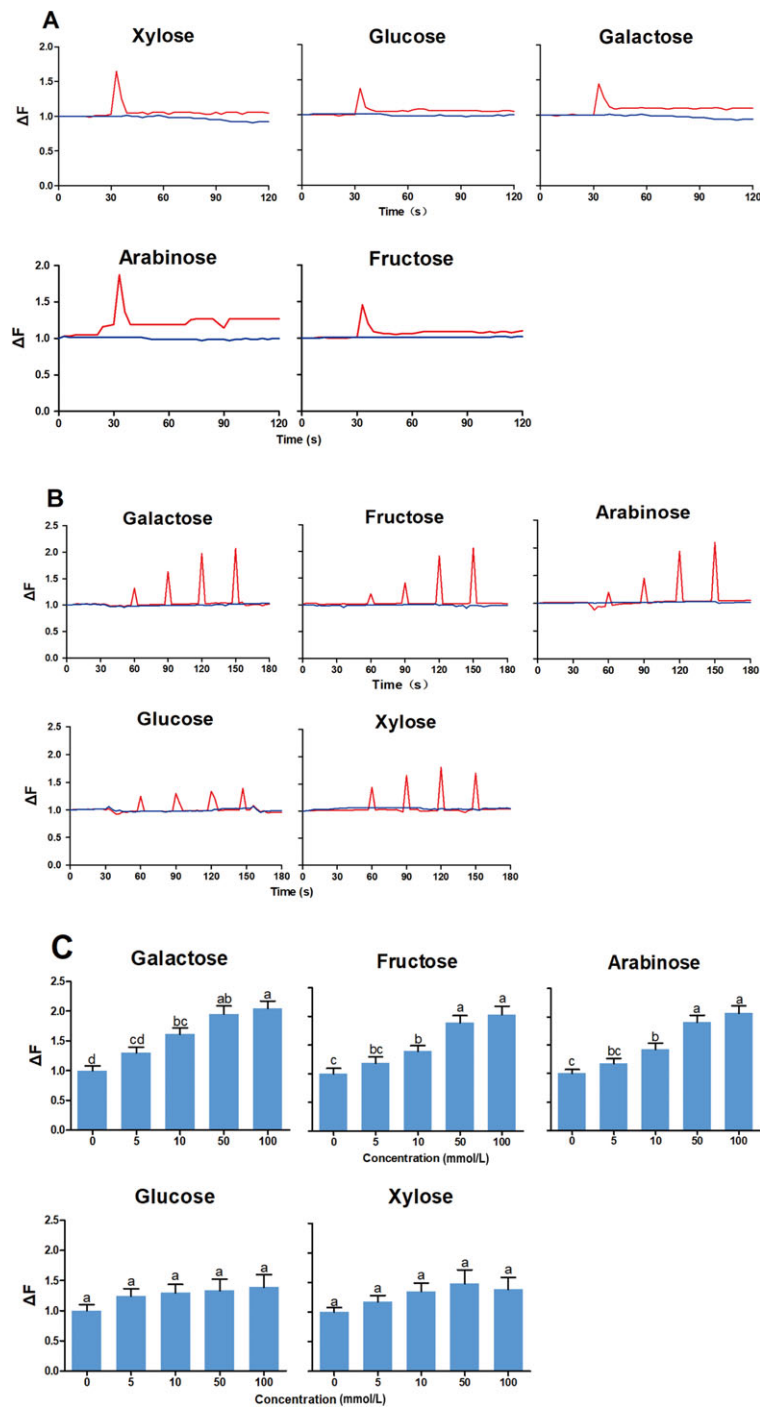
Fig. 3 Ca-dependent response to sugar stimulants in *Sf*9 cells expressing *NlGr11* genes. (A) ΔF elicited by various sugar solutions. A 0.2 mL test solution (10 mmol/L) was pulsed for 3 s to a glass-bottom cell culture dish containing 2 mL cell culture for the 30 s (*Nl*Gr11/pIZ-V5 cells: red lines; pIZ-V5 cells: blue lines). ΔF represents the level of intracellular Ca^{2+}; the value was set to 1 before the addition of the compound. (B) ΔF elicited by five preliminary sugar ligand solutions. Following the order 0, 5, 10, 50 and 100 mmol/L, five preliminary sugar ligands were added into the same dish of cells every 30 s. (C) ΔF elicited by five preliminary sugar ligand solutions. Following the order 0, 5, 10, 50 and 100 mmol/L, five preliminary sugar ligands were added into different dishes of cells every 30 s. The data represent means + SEM ($n = 10$). Different lower-case letters above columns represent significant differences ($P < 0.05$, Duncan's multiple range test).
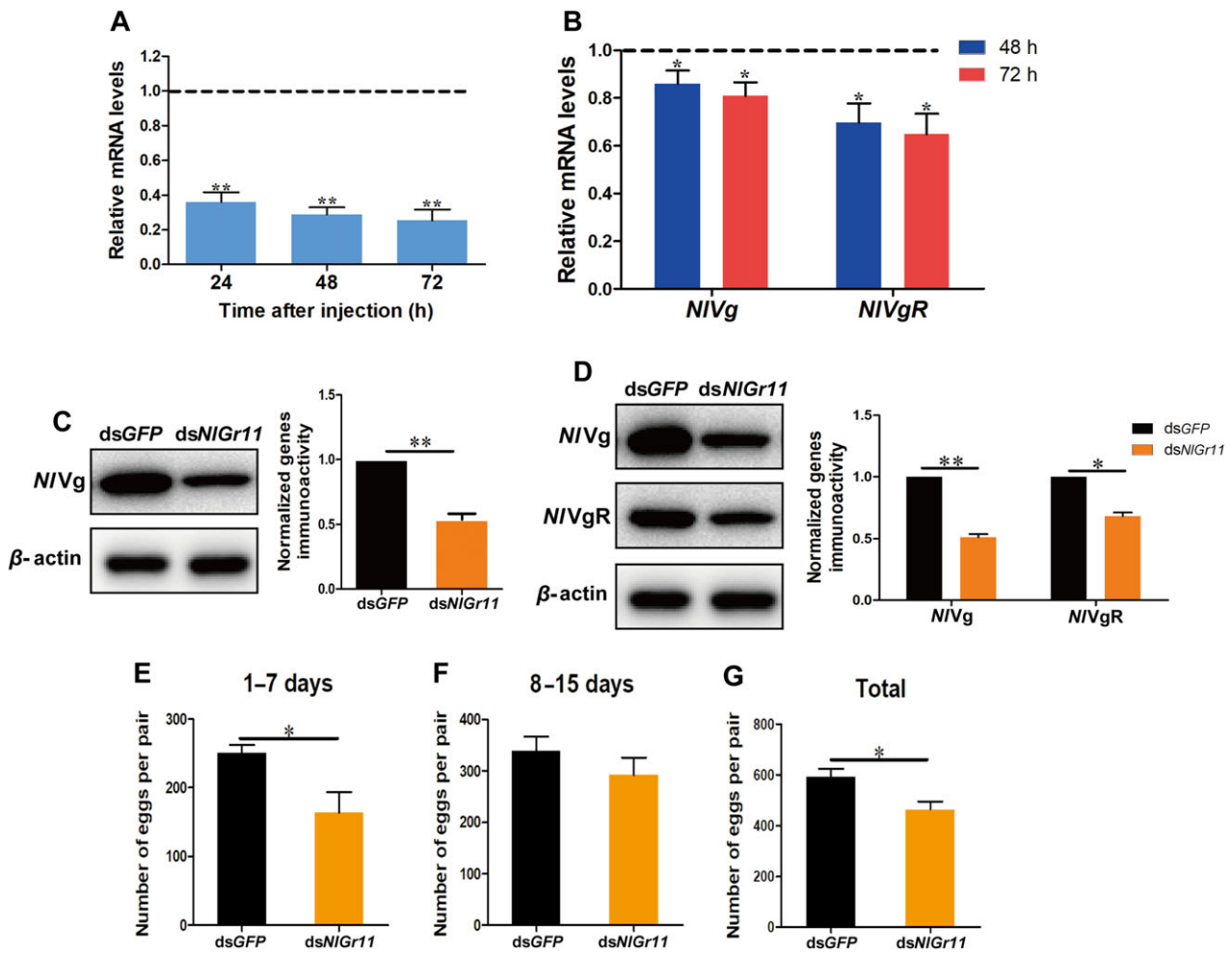
Fig. 4 The effect of *Nl*Gr11 on fecundity of brown planthoppers (BPH). The messenger RNA (mRNA) levels of *Nl*Gr11 in whole bodies (A), *Nl*Vg in fat bodies and *Nl*VgR in ovaries (B) after injection of *Nl*Gr11 double-stranded RNA (dsRNA). All mRNA levels were normalized relative to the β-actin mRNA levels. The mRNA level of ds*GFP* was set to 1. The protein levels of *Nl*Vg in fat bodies (C) and the protein levels of *Nl*Vg and *Nl*VgR in ovaries (D) at 72 h after injection of *Nl*Gr11 dsRNA. The average of the ds*GFP* was set to 1. The number of eggs for 1–7 days (E), 8–15 days (F) and all 15 days (G) after injection of *Nl*Gr11 dsRNA. The data represent means + SEM ($n = 3$), *$P < 0.05$, **$P < 0.01$, t-test.

analysis of RNA isolated from females at 24 h, 48 h and 72 h after injection. The results showed that the mRNA levels of *Nl*Gr11 were significantly decreased at 24 h, 48 h and 72 h after injection (Fig. 4A). This finding suggested that the RNA interference (RNAi) of *Nl*Gr11 was successful. Subsequently, we examined the effect of *Nl*Gr11 on the fecundity of BPH. Because *Nl*Vg and *Nl*VgR are molecular markers of fecundity in BPH (Fu *et al.*, 2015; Qiu *et al.*, 2016; Pang *et al.*, 2017), we first measured the expression levels of *Nl*Vg and *Nl*VgR after the injection of *Nl*Gr11 dsRNA. For *Nl*Vg, both the mRNA levels in fat bodies (Fig. 4B) and the protein levels in fat bodies (Fig. 4C) and ovaries (Fig. 4D) were decreased significantly after inhibition of *Nl*Gr11 expression; for *Nl*VgR, both the

mRNA levels (Fig. 4B) and the protein levels (Fig. 4D) in ovaries were also significantly decreased. These results confirmed that *Nl*Gr11 modulates the fecundity of BPH.

Thus, we measured the number of eggs laid by BPHs between 1–7 days and 8–15 days after injection of *Nl*Gr11 dsRNA. We found a significant reduction in the number of eggs between 1 and 7 days after knockdown of *Nl*Gr11 compared with the control (injected with *GFP* dsRNA) (Fig. 4E) and no significant difference between 8 and 15 days (Fig. 4F). However, the number of eggs laid over all 15 days was still significantly less than that of the control (Fig. 4G). These results further confirmed that *Nl*Gr11 promotes the fecundity of BPH.

Molecular mechanism by which NlGr11 modulates fecundity in BPH

The gene expression of Vg was affected by at least four signaling pathways, including the insulin pathway, the nutrition-related target of rapamycin (TOR) pathway, the ecdysone and juvenile hormone pathway and an energy-related pathway (Qiu *et al.*, 2016). To uncover the possible molecular mechanism by which *Nl*Gr11 modulates the fecundity of BPH, nine genes in those four signaling pathways, namely, *AMPK*, *AKT*, *TOR*, S6 Kinase (*S6K*), Forkhead Box Protein O (*FoxO*), Glutamine Synthetase (*GS*), Ecdysone Receptor (*EcR*), Methoprene Tolerant (*Met*) and Broad Complex (*Br-C*), were chosen for measurement of their expression levels after inhibition of *NlGr11* expression. According to the interference efficiency of *NlGr11*, the mRNA levels were measured at 48 h and 72 h post-injection. We found that the mRNA levels of *AMPK* and *Met* were significantly increased; those of *AKT*, *TOR*, *EcR* and *Br-C* were significantly decreased; and those of *GS*, *S6K* and *FoxO* showed no significant difference (Fig. 5A). Because AMPK and AKT are the

key kinases in energy metabolism and insulin/insulin-like peptide signaling pathways, respectively (Hardie *et al.*, 2003; Manning & Cantley, 2007), we further measured their phosphorylation. We found that the phosphorylation level of AMPK significantly increased and the phosphorylation level of AKT significantly decreased after inhibition of *NlGr11* expression (Fig. 5B). These results showed that *Nl*Gr11 modulates the phosphorylation of AMPK and AKT in opposite manners.

To investigate the effects of AMPK and AKT on the fecundity of BPH, we examined the gene expression levels of *NlVg* and *NlVgR* and the number of eggs laid after injecting *AMPKα* dsRNA and *AKT* dsRNA into 1-day-old females. Similarly, we found that inhibition of *AMPKα* and *AKT* expression was successful (Fig. 6A); the mRNA and the protein levels of *Nl*Vg and *Nl*VgR and the number of eggs increased significantly after inhibition of *AMPKα*, while the mRNA and the protein levels of *Nl*Vg and *Nl*VgR and the number of eggs decreased significantly after inhibition of *AKT* (Fig. 6). These results showed that AMPK and AKT also modulate the fecundity of BPH in opposite manners.
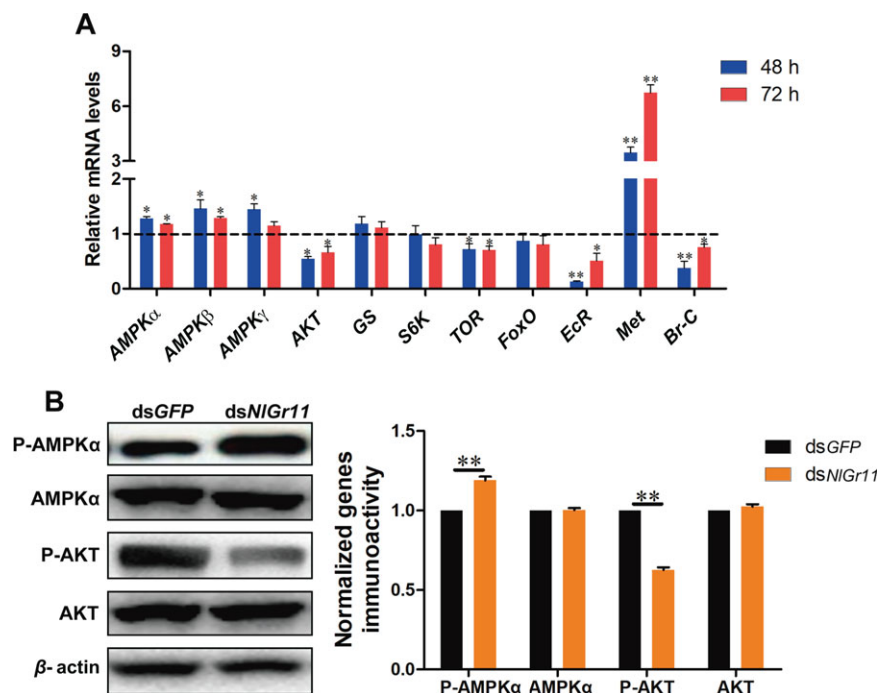

Fig. 5 The effect on various genes after RNA interference (RNAi) *NlGr11*. (A) The messenger RNA (mRNA) expression levels of nine genes that affect Vg expression. All mRNA levels were normalized relative to the *β*-actin mRNA levels. The mRNA level of ds*GFP* was set to 1. (B) The phosphorylation levels and protein levels of adenosine monophosphate-activated protein kinase *α* (AMPK*α*) and protein kinase B (AKT) in whole body at 72 h after injection of *NlGr11* dsRNA. The average of the ds*GFP* was set to 1. The data represent means + SEM ($n = 3$), *$P < 0.05$, **$P < 0.01$, *t*-test.
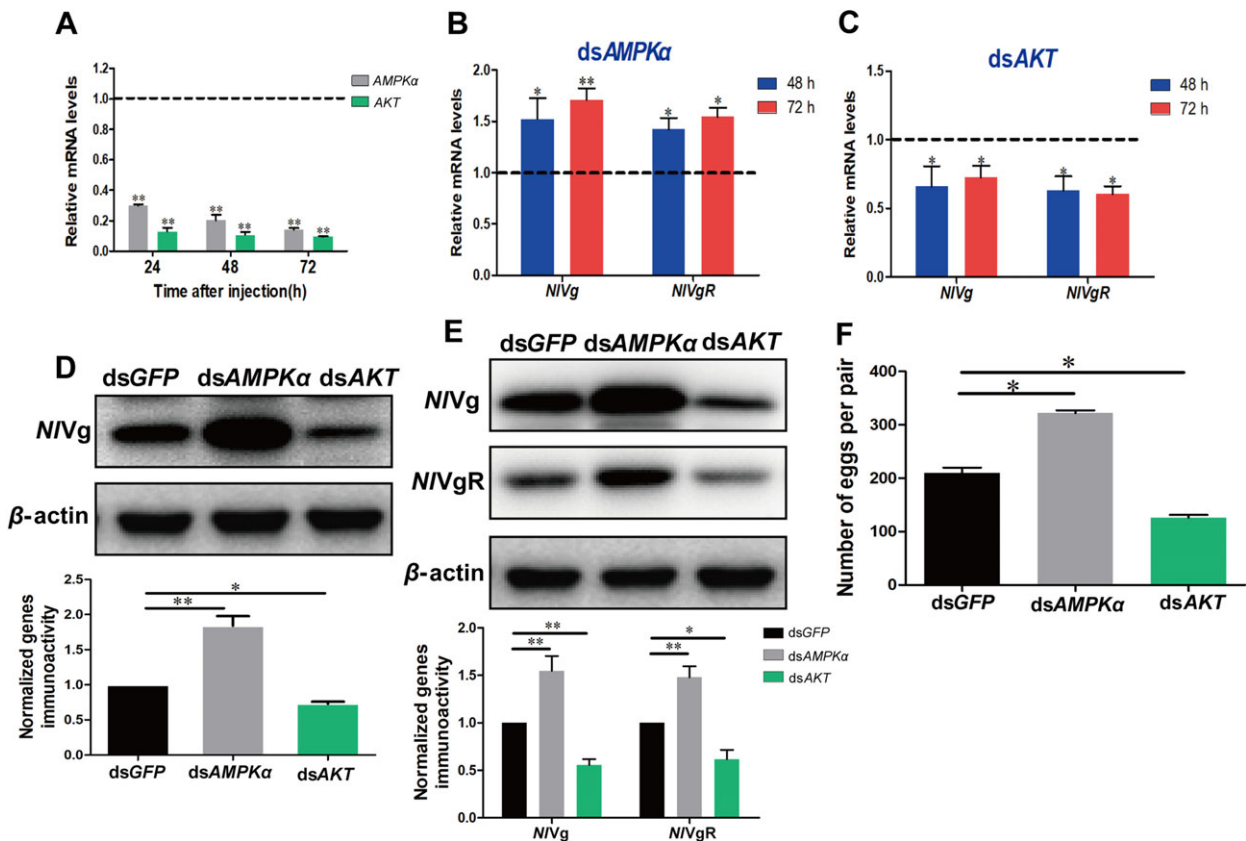
Fig. 6 The effect of adenosine monophosphate-activated protein kinase (AMPK) and protein kinase B (AKT) on fecundity of brown plant hopper (BPH). The messenger RNA (mRNA) levels of *AMPKα* and *AKT* after inhibition of *AMPKα* and *AKT* (A), *NlVg* in fat bodies and *NlVgR* in ovaries after inhibition of *AMPKα* (B) and *AKT* (C). All mRNA levels were normalized relative to the *β*-actin mRNA levels. The mRNA level of ds*GFP* was set to 1. (D) The protein levels of *Nl*Vg in fat bodies and (E) the protein levels of *Nl*Vg and *Nl*VgR in ovaries at 72 h after injection of *AMPKα* dsRNA and *AKT* dsRNA. The average of the ds*GFP* was set to 1. (F) The number of eggs for 1–7 days after inhibition of *AMPKα* and *AKT*. The data represent means + SEM ($n = 3$), $*P < 0.05$, $**P < 0.01$, *t*-test.

Discussion

In *D. melanogaster*, the ligands of most gustatory receptors have been identified through a combination of electrophysiology and behavioral genetic analyses. However, it is to some extent difficult to accurately interpret electrophysiological recordings and behaviors between wild-type and Gr mutant flies (Miyamoto *et al.*, 2013). Ca^{2+} influx and Ca^{2+} imaging assay have often been used to identify ligands of gustatory receptors in other insects (Ozaki *et al.*, 2011; Sato *et al.*, 2011). The measurement of ligand-induced calcium responses was based on the detection of an increase in the fluorescence of cells preloaded with a calcium-sensitive fluorescent dye (e.g. Fura-2/AM) (Sato *et al.*, 2011), a Ca-dependent luminescence protein (e.g. Aequorin) (Torfs *et al.*, 2002) or a Ca^{2+} sensitive fluorescent reporter (e.g. GCaMP3.0)

(Miyamoto *et al.*, 2013). The method for preloading cells with Fura-2/AM was used to identify the ligand of *Nl*Gr11 in this study. For sugar receptors, sugar-activated Ca^{2+} influx may take place through ionotropic sugar receptors, cyclic nucleotide-gated cation channels, and/or voltage-gated cation channels (Murata *et al.*, 2006). The transduction pathways, including G proteins and IP_3 channel pathways, have been demonstrated in sugar receptors of some insects (Koganezawa & Shimada, 1997, 2002; Ahamed *et al.*, 2002). In many cell types, G protein-coupled receptors, gustatory receptors coupling to G protein *α* subunits leads to a temporal increase in the intracellular calcium concentration as a result of IP_3-activated release of calcium ions from intracellular stores (Torfs *et al.*, 2002). Therefore, we suppose that ligand-activated Ca^{2+} influx may take place through a G protein-IP_3-Ca^{2+} pathway.
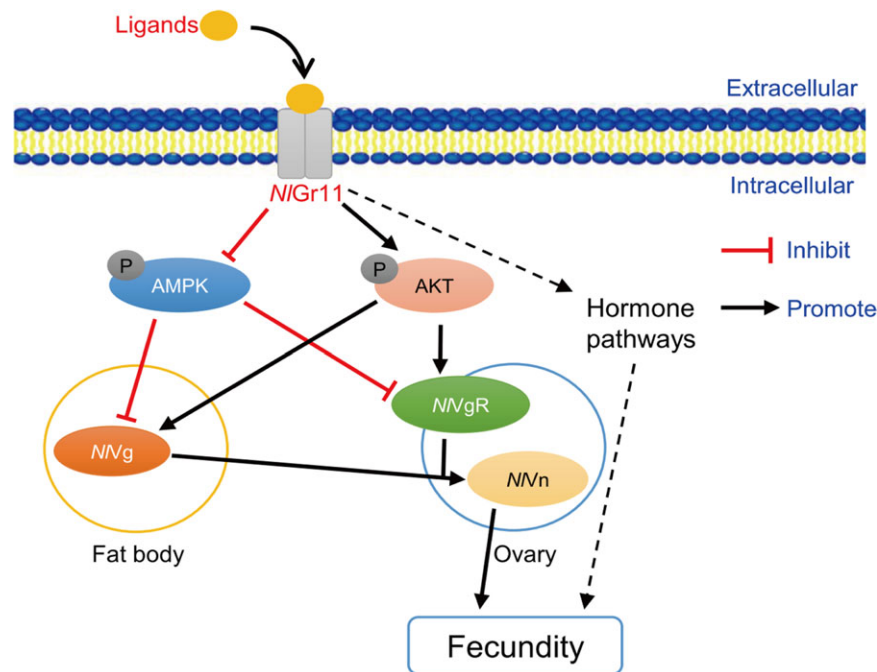
Fig. 7 Proposed model of *Nl*Gr11 accelerate fecundity of brown planthopper (BPH) through adenosine monophosphate-activated protein kinase (AMPK)- and AKT-mediated signaling pathways.

Because *Nl*Gr11 is a sugar gustatory receptor, we used 12 sugars to determine the receptor's ligands. The results showed that fructose, glucose, galactose, arabinose and xylose caused an increase in intracellular Ca^{2+} levels (Fig. 3A, Fig. S3). Because the combination of sugar gustatory receptors and their ligands can cause a dose-dependent response (Sato *et al.*, 2011; Miyamoto *et al.*, 2012), we conducted a second round of selection by using different concentrations of those five sugars and found that only fructose, galactose and arabinose caused a dose-dependent response (Fig. 3B). Moreover, these three sugars showed a saturable response (Fig. 3C), in accordance with the saturable characteristic of the combination of ligands and receptors. Thus, these results confirmed that fructose, galactose and arabinose are ligands of *Nl*Gr11. Glucose and xylose can also cause an increase in intracellular Ca^{2+} levels in *Nl*Gr11-*Sf*9 cells, we assume that the expression of *Nl*Gr11 in *Sf*9 cells may promote the expression, localization, or function of the endogenous gustatory receptors of *Sf*9 cells, thus leading to the higher responses to glucose and xylose. This finding is similar to the lower response to trehalose observed when expressing HaGR9 in *Sf*9 cells (Xu *et al.*, 2012).

To date, little is known about the physiological functions of insect sugar receptors. The only example, Gr43a in *D.*

melanogaster, was proven to promote feeding in hungry flies but to suppress feeding in satiated flies (Miyamoto *et al.*, 2012). In this study, we found that *Nl*Gr11 accelerated the fecundity of BPH. To our knowledge, this is the first time that a relationship between gustatory receptors and the fecundity of insects has been observed. We found the number of eggs laid by BPH decreased significantly after injection of *Nl*Gr11dsRNA, although this effect lasted for only a few days (Fig. 3), because the effect of RNAi is often not sufficiently strong after a certain period following treatment (Yang *et al.*, 2001).

Our data demonstrate that *Nl*Gr11 accelerates the fecundity of BPH through AMPK- and AKT-mediated signaling pathways (Fig. 7). On the one hand, *Nl*Gr11 inhibits phosphorylation of AMPK, it induces promoting the synthesis of *Nl*Vg in fat bodies and the synthesis of *Nl*VgR in ovaries. Higher levels of *Nl*Vg and uptaking into oocytes by *Nl*VgR together induce more Vitellin (Vn), which results in more eggs. On the other hand, *Nl*Gr11 promotes phosphorylation of AKT, it also promotes the synthesis of *Nl*Vg and *Nl*VgR, then finally promotes the fecundity of BPH. Moreover, the mRNA expression level of *Met* was extremely increased while the mRNA expression levels of *EcR* and *Br-C* were extremely reduced when the expression of *Nl*Gr11 was down-regulated (Fig. 5A). Our previous study showed that the number of offspring of BPH

decreased significantly after inhibition of *EcR* expression (Yu *et al.*, 2014). We suppose that *Nl*Gr11 binding with its ligands may activate hormone pathways and afterwards modulate the fecundity of BPH (Fig. 7).

In summary, we identified the ligands of *Nl*Gr11, including fructose, galactose and arabinose, and found that *Nl*Gr11 modulated BPH fecundity through AMPK- and AKT-mediated signaling pathways. These findings broaden our understanding of the functions of sugar gustatory receptors in insects.

Acknowledgments

Disclosure

The authors declare that they have no conflicts of interest with respect to the contents of this article.

References

Ahamed, A., Tsurumi, S. and Amakawa, T. (2002) Triterpenoid saponins stimulate the sugar taste receptor cell through a G protein-mediated mechanism in the blowfly, *Phormia regina. Journal of Insect Physiology*, 48, 367–374.

Briscoe, A.D., Macias-Muñoz, A., Kozak, K.M., Walters, J.R., Yuan, F.R., Jamie, G.A. *et al*. (2013) Female behaviour drives expression and evolution of gustatory receptors in butterflies. *PLoS Genetics*, 9, e1003620.

Chen, J., Liang, Z.K., Liang, Y.K., Pang, R. and Zhang, W.Q. (2013) Conserved microRNAs miR-8-5p and miR-2a-3p modulate chitin biosynthesis in response to 20-hydroxyecdysone signaling in the brown planthopper, *Nilaparvata lugens. Insect Biochemistry and Molecular Biology*, 43, 839–848.

Clyne, P.J., Warr, C.G. and Carlson, J.R. (2000) Candidate taste receptors in *Drosophila*. *Science*, 287, 1830–1834.

Dahanukar, A., Foster, K., van der Goes van Naters W.M. and Carlson, J.R. (2001) A Gr receptor is required for response to the sugar trehalose in taste neurons of *Drosophila. Nature Neuroscience*, 4, 1182–1186.

Dong, J.F., Song, Y.Q., Li, W.L., Shi, J. and Wang, Z.Y. (2016) Identification of putative chemosensory receptor genes from the *Athetis dissimilis* antennal transcriptome. *PLoS ONE*, 11, e0147768.

Freeman, E.G., Wisotsky, Z. and Dahanukar, A. (2014) Detection of sweet tastants by a conserved group of insect gustatory receptors. *Proceedings of the National Academy of Sciences USA*, 111, 1598–1603.

Fu, X., Li, T.C., Chen, J., Dong, Y., Qiu, J.Q., Kang, K. *et al*. (2015) Functional screen for microRNAs of *Nilaparvata lugens* reveals that targeting of glutamine synthase by mir-4868b regulates fecundity. *Journal of Insect Physiology*, 83, 22–29.

Ge, X., Zhang, T.T., Wang, Z.Y., He, K.L. and Bai, S.X. (2016) Identification of putative chemosensory receptor genes from yellow peach moth *Conogethes punctiferalis* (Guenée) antennae transcriptome. *Scientific Reports*, 6, 32636.

Guo, H.Z., Cheng, T.C., Chen, Z.W., Jiang, L., Guo, Y.B., Liu, J.Q. *et al*. (2017) Expression map of a complete set of gustatory receptor genes in chemosensory organs of *Bombyx mori. Insect Biochemistry and Molecular Biology*, 82, 74–82.

Hardie, D.G., Scott, J.W., Pan, D.A. and Hudson, E.R. (2003) Management of cellular energy by the AMP-activated protein kinase system. *FEBS Letters*, 546, 113–120.

Jena, K.K. and Kim, S.M. (2010) Current status of brown planthopper (BPH) resistance and genetics. *Rice*, 3, 161–171.

Jiao, Y.C., Moon, S.J. and Montell, C. (2007) A *Drosophila* gustatory receptor required for the responses to sucrose, glucose, and maltose identified by mRNA tagging. *Proceedings of the National Academy of Sciences USA*, 104, 14110–14115.

Jung, J.W., Park, K.W., Ahn, Y.J. and Kwon, H.W. (2015) Functional characterization of sugar receptors in the western honeybee, *Apis mellifera. Journal of Asia-Pacific Entomology*, 18, 19–26.

Kang, Z.W., Tian, H.G., Li, F.H., Liu, X., Jing, X.F. and Liu, T.-X. (2017) Identification and expression analysis of chemosensory receptor genes in an aphid endoparasitoid *Aphidius gifuensis. Scientific Reports*, 7, 3939.

Kent, L.B., Walden, K.K.O. and Robertson, H.M. (2008) The Gr family of candidate gustatory and olfactory receptors in the yellow-fever mosquito, *Aedes aegypti. Chemical Senses*, 33, 79–93.

Koganezawa, M. and Shimada, I. (1997) The effects of G protein modulators on the labellar taste receptor cells of the fleshfly (*Boettcherisca peregrina*). *Journal of Insect Physiology*, 43, 225–233.

Koganezawa, M. and Shimada, I. (2002) Inositol 1,4,5-trisphosphate transduction cascade in taste reception of the fleshfly, *Boettcherisca peregrina. Journal of Neurobiology*, 51, 66–83.

Lee, Y., Sang, H.K. and Montell, C. (2010) Avoiding DEET through insect gustatory receptors. *Neuron*, 67, 555–561.

Manning, B.D. and Cantley, L.C. (2007) AKT/PKB signaling: navigating downstream. *Cell*, 129, 1261–1274.

Mitsumasu, K., Azuma, M., Niimi, T., Yamashita, O. and Yag-
inuma, T. (2008) Changes in the expression of soluble and
integral-membrane trehalases in the midgut during meta-
morphosis in *Bombyx mori. Zoological Science*, 25, 693–
698.

Miyamoto, T., Chen, Y., Slone, J. and Amrein, H. (2013) Identi-
fication of a *Drosophila* glucose receptor using Ca^{2+} imaging
of single chemosensory neurons. *PLoS ONE*, 8, e56304.

Miyamoto, T., Slone, J., Song, X.Y. and Amrein, H. (2012)
A fructose receptor functions as a nutrient sensor in the
Drosophila brain. *Cell*, 151, 1113–1125.

Murata, Y., Ozaki, M. and Nakamura, T. (2006) Primary cul-
ture of gustatory receptor neurons from the blowfly *Phormia
regina. Chemical Senses*, 31, 497–504.

Ni, L., Bronk, P., Chang, E.C., Lowell, A.M., Flam, J.O., Pan-
zano, V.C. *et al.* (2013) A gustatory receptor paralogue con-
trols rapid warmth avoidance in *Drosophila. Nature*, 500,
580–584.

Ozaki, K., Ryuda, M., Yamada, A., Utoguchi, A., Ishimoto, H.,
Calas, D. *et al.* (2011) A gustatory receptor involved in host
plant recognition for oviposition of a swallowtail butterfly.
Nature Communications, 2, 542.

Pang, R., Qiu, J.Q., Li, T.C., Pan, Y.X., Yue, L., Yang, P. *et al.*
(2017) The regulation of lipid metabolism by a hypothetical
P-loop NTPase and its impact on fecundity of the brown plan-
thopper. *Biochimica et Biophysica Acta-General Subjects*,
1861, 1750–1758.

Qiu, J.Q., He, Y., Zhang, J.Q., Kang, K., Li, T.C. and Zhang, W.Q.
(2016) Discovery and functional identification of fecundity-
related genes in the brown planthopper by large-scale RNA
interference. *Insect Molecular Biology*, 25, 724–733.

Robertson, H.M. and Wanner, K.W. (2006) The chemoreceptor
superfamily in the honey bee, *Apis mellifera*: expansion of the
odorant, but not gustatory, receptor family. *Genome Research*,
16, 1395–1403.

Sato, K., Tanaka, K. and Touhara, K. (2011) Sugar-regulated
cation channel formed by an insect gustatory receptor. *Pro-
ceedings of the National Academy of Sciences USA*, 108,
11680–11685.

Scott, K., Brady, R.J., Cravchik, A., Morozov, P., Rzhetsky, A.,
Zuker, C. *et al.* (2001) A chemosensory gene family encoding
candidate gustatory and olfactory receptors in *Drosophila.
Cell*, 104, 661–673.

Shim, J., Lee, Y., Jeong, Y.T., Kim, Y., Lee, M.G., Montell,
C. *et al.* (2015) The full repertoire of *Drosophila* gustatory
receptors for detecting an aversive compound. *Nature Com-
munications*, 6, 8867.

Torfs, H., Poels, J., Detheux, M., Dupriez, V., Van, L.T., Ver-
cammen, L. *et al.* (2002) Recombinant aequorin as a reporter
for receptor-mediated changes of intracellular Ca^{2+}-levels
in *Drosophila* S2 cells. *Invertebrate Neuroscience*, 4, 119–
124.

Xu, W., Papanicolaou, A., Zhang, H.J. and Anderson, A. (2016)
Expansion of a bitter taste receptor family in a polyphagous
insect herbivore. *Scientific Reports*, 6, 23666.

Xu, W., Zhang, H.J. and Anderson, A. (2012) A sugar gustatory
receptor identified from the foregut of cotton bollworm *He-
licoverpa armigera. Journal of Chemical Ecology*, 38, 1513–
1520.

Yang, S.C., Tutton, S., Pierce, E. and Yong, K. (2001) Specific
double-stranded RNA interference in undifferentiated mouse
embryonic stem cells. *Molecular and Cellular Biology*, 21,
7807–7816.

Yu, R., Xu, X.P., Liang, Y.K., Tian, H.G., Pan, Z.Q., Jin, S.H.
et al. (2014) The insect ecdysone receptor is a good potential
target for RNAi-based pest control. *International Journal of
Biological Sciences*, 10, 1171–1180.

Zhang, H.J., Anderson, A.R., Trowell, S.C., Luo, A.R., Xiang,
Z.H. and Xia, Q.Y. (2011) Topological and functional char-
acterization of an insect gustatory receptor. *PLoS ONE*, 6,
e24111.

Supporting Information

Additional Supporting Information may be found in the
online version of this article at the publisher's web-site:

Fig. S1. Nucleotide and deduced amino acid sequences
of *Nl*Gr11 cDNA. The prediction of seven transmembrane
regions is underlined with solid lines. *Represents the
terminal codon.

Fig. S2. *Nl*Gr11 expressed in *Sf*9 cells. (A) *Nl*Gr11 ex-
pressed in *Sf*9 cell membrane. The cells were observed
under confocal laser scanning microscope positioning us-
ing Hoehst 33342 dye labeled nuclei. Merge synthesis in
front of the two maps. (B) Detection protein expression
by anti-*Nl*Gr11 after extracting cell membrane protein.
After transfection for 60 h, the membrane protein was
extracted (Lower: Lower extract; Upper: Upper extract),
and the nontransfected cells were used as CK, the plasmid
transfected cell as a control group.

Fig. S3. Ca-dependent response to sugar stimulants in
*Sf*9 cells expressing *NlGr11* genes. ΔF elicited by various
sugar solutions. A 0.2 mL test solution (10 mmol/L) was
pulsed for 3 s to a glass-bottom cell culture dish contain-
ing 2 mL cell culture for 30 s (*Nl*Gr11/pIZ-V5 cells: red
lines; pIZ-V5 cells: blue lines). ΔF represents the level
of intracellular Ca^{2+}; the value was set to 1 before the
addition of the compound.

Table S1. The primers used in this study.